Synthesis and Characterization of Graphene-Containing Thermoresponsive Nanocomposite Hydrogels of Poly(*N*-vinylcaprolactam) Prepared by Frontal Polymerization

Roberta Sanna,[1] Davide Sanna,[1] Valeria Alzari,[1] Daniele Nuvoli,[1] Sergio Scognamillo,[1] Massimo Piccinini,[2] Massimo Lazzari,[3] Emilia Gioffredi,[4] Giulio Malucelli,[4] Alberto Mariani[1]

[1]Dipartimento di Chimica e Farmacia, Università di Sassari, and local INSTM Unit, Via Vienna 2, 07100 Sassari, Italy
[2]Porto Conte Ricerche S.r.l., SP 55 km 8.400 Loc. Tramariglio, 07041 Alghero, Sassari, Italy
[3]Centre for Research in Biological Chemistry and Molecular Materials (CIQUS), University of Santiago de Compostela, 15782 Santiago de Compostela, Spain
[4]Dipartimento di Scienza Applicata e Tecnologia, Politecnico di Torino, sede di Alessandria, and local INSTM unit, Via T. Michel 5,15121 Alessandria, Italy
Correspondence to: G. Malucelli (E-mail: giulio.malucelli@polito.it) or A. Mariani (E-mail: mariani@uniss.it)

Received 19 April 2012; accepted 8 June 2012; published online 5 July 2012
DOI: 10.1002/pola.26215

ABSTRACT: Thermoresponsive poly(*N*-vinylcaprolactam) nanocomposite hydrogels containing graphene were successfully prepared by frontal polymerization. High concentration of graphene (5.0 mg/mL) was obtained by direct graphite sonication in the self-same liquid monomer, thus avoiding any chemical manipulation and obtaining "real" graphene as nanofiller instead of one of its more or less oxidized derivative, which is what generally reported in published reports. Furthermore, the corresponding nanocomposites were obtained without using any solvent to be eventually removed. The materials were fully characterized by RAMAN, SEM, and TEM, and their swelling behavior and rheological properties were investigated. © 2012 Wiley Periodicals, Inc. J Polym Sci Part A: Polym Chem 50: 4110–4118, 2012

KEYWORDS: frontal polymerization; graphene; hydrogels; nanocomposites, stimuli-sensitive polymers

INTRODUCTION Polymer hydrogels are highly crosslinked materials having a tridimensional and flexible structure, able to swell when they are immersed in aqueous solutions. Indeed, chemical or physical crosslinking avoids their solubilization, since water can penetrate through the network without breaking the strong interactions that bind the polymer chains. The extent of the swelling is modulated by the nature of the monomers: hydrogels containing hydrophilic functional groups, which are able to establish hydrogen bonds with water molecules, swell more than those containing hydrophobic groups, which tend to minimize the interactions with the solvent.[1]

In the latest years, a particular class of polymer hydrogels has been characterized by increasing interest: the so-called *smart* or *stimuli responsive* hydrogels, which are able to contract or swell their structures as a function of external stimuli such as temperature, pH, ionic force, pressure, mechanical stress, electric, and magnetic field. These unique characteristics are of great interest, for example, in biomedical and pharmaceutical field for artificial tendons and tissues,[2] contact lens,[3] controlled drug delivery.[4–7] Stimuli responsive hydrogels have also found application in bulk engineering and microscale medicine, in particular for microfluidic devices,[8] pulsate drug release systems,[9,10] motors/actuators,[11] and bioadhesion mediators.[12,13]

More specifically, temperature responsive hydrogels are materials that show a volume change at a certain temperature, at which a sharp alteration in the solvation state occurs: a small temperature variation across the critical solution temperature (CST) results in contraction or expansion of the polymer chain structure, as a consequence of the optimization of the hydrophobic and hydrophilic interactions between polymer chains and aqueous solution.

The CST, at which the volume phase transition occurs, is therefore an important parameter for describing thermoresponsive polymer systems. Polymer hydrogels that are deswollen below a given temperature exhibit an upper critical solution temperature (UCST) while a lower critical solution temperature (LCST) characterizes those that are swollen below a given temperature. Some particular hydrogels can exhibit both UCST and LCST: these materials swell when they are heated up to temperature above UCST or are cooled

down below LCST, whereas they contract when the temperature is in between UCST and LCST.

The most popular thermoresponsive polymer hydrogel is poly(*N*-isopropylacrylamide), PNIPAAm, which possesses a sharp phase transition in water at around 32–33°C.[14] This temperature, extremely close to the physiological one, makes this material suitable for such biomedical and pharmaceutical applications as embolic agents[15] and for drug delivery systems.[16–18]

Poly(*N*-vinylcaprolactam), PNVCL, is another thermoresponsive polymer hydrogel that is attracting great interest;[19–22] it belongs to the same family of poly(vinylpyrrolidone), PVP, which is widely used for pharmaceutical or biomedical purposes.[23] PNVCL is a non-ionic polymer, soluble in aqueous environmental, and, similarly to PVP, able to absorb a large number of organic compounds from water.[24,25] It is also a very interesting material because of its stability against hydrolysis, which makes it more biocompatible than PNIPAAm.[26–29] In addition, it exhibits an LCST at about 32–34°C making it a valid alternative to PNIPAAm in a controlled drug-delivery systems,[30,31] in the immobilization of enzymes,[32] and in separation science.[33]

Despite of these features, the mechanical properties of the above hydrogels are often quite poor, thus limiting the number of their possible applications. For such a reason, part of the research efforts in this field is devoted to the preparation of nanocomposite hydrogels, including those containing layered silicates,[34,35] metals,[36–39] magnetic particles,[40,41] and graphene.[42]

In recent years, among the various nanoparticles, graphene has been largely studied for its outstanding features. Graphene is a planar monolayer of sp^2-hybridized carbon atoms arranged into a two-dimensional honeycomb lattice, with a carbon—carbon bond length of 0.142 nm.[43] When compared with the other allotropic forms of carbon, this material exhibits its peculiar characteristics that are object of study and development in all the most advanced technological fields. For this reason, over the past decade, the interest of the scientific community toward this innovative material has increased exponentially. Indeed, graphene is characterized by high electron mobility at room temperature (250000 cm^2/Vs),[44–46] extraordinary thermal[46] and electric conductivity[46] (5000 W/m × K and 0.96 × 10^6 Ω^{-1} × cm^{-1} respectively), high Young modulus (1 TPa[46]), and tensile strength (higher than steel, 42 N/m^2).[46] All these features make graphene one of the best candidates for numerous applications for functional devices such as energy storage systems,[47] photovoltaics,[48] field-effect transistors,[49] gas sensor,[50] and transparent conducting electrodes,[51] and polymer nanocomposites.[42,52]

Lately, several routes for graphene production have been developed, including mechanical exfoliation,[46] chemical vapor deposition,[53–55] reduction of CO,[56] chemical conversion,[57–61] epitaxial growth on crystalline silicon carbide,[62] unzipping of carbon nanotubes,[63,64] and arc discharge.[65,66] Although most of these techniques afford to obtain a defect-free graphene, they are characterized by a low productivity, which makes them unsuitable for the industrial applications.[57]

On the other hand, the methods based on the obtainment of graphene from colloidal suspensions have many advantages, such as high yields and simple protocols: among them, the most important are the chemical oxidation of graphite to graphite oxide and its subsequent reduction to graphene after exfoliation,[67] and the direct ultrasonic exfoliation of graphite in organic solvents without any chemical modification.[42,52,67–69]

However, even though the first route is being largely exploited, it involves the formation of carboxy and alkoxy groups on the edges, and of epoxy groups on the basal plane of the graphene sheets. Graphene oxide is then reduced to "graphene." Nevertheless, only the epoxy groups are actually reduced, unlike carboxy and alkoxy functionalities: in other words, most of the "so-called graphene" reported in published reports still exhibits a large number of impurities that influence its chemical and physical characteristics.

At variance, Coleman and colleagues opened a new route for obtaining graphene by direct graphite exfoliation in *N*-methylpyrrolidone (NMP), thus avoiding any chemical manipulation and initially achieving a concentration of 0.01 mg/mL.[67] Our research group successfully developed a similar method for obtaining graphene dispersions having the highest concentrations achieved so far in any liquid and, for the first time, also directly in the monomer. Indeed, we were able to disperse graphene in different media, such as 1-hexyl-3-methylimidazolium hexafluorophosphate[67] (graphene concentration: 5.33 mg/mL), NMP[42] (2.21 mg/mL), and tetraethyleneglycoldiacrylate[52] (9.45 mg/mL). When compared with the other techniques, our method involves a simpler protocol, lower energy consumption and the obtainment of graphene without any processing-induced defect. However, at variance to some of the more sophisticated methods aforementioned, the use of common graphite, which is characterized by flakes having a large size distribution, results in graphene sheets having various shapes and size. As reported in our previous study, this is not inconvenient for preparing polymer nanocomposites.[42,52]

Frontal polymerization (FP) is an alternative synthetic technique that exploits the heat released during the polymerization reaction for promoting the formation of a hot front that can sustain itself and propagate throughout the reactor, thus converting monomer into polymer. FP is a very simple and economic route characterized by short-reaction times and low-energy consumption.

This method was proposed for the first time by Chechilo and Enikolopyan, who applied FP to methyl methacrylate.[70,71] Lately, Pojman et al. exploited FP for polymerizing different vinyl monomers,[72–74] epoxy resins,[75,76] ionic liquids,[77] interpenetrating polymer networks,[78] and poly(dicyclopentadiene).[79] Chen et al. frontally polymerized 2-hydroxyethyl acrylate[80] and methyloacrylamide;[81] furthermore, they exploited this technique for obtaining epoxy resin/polyurethane networks,[82] and poly(*N*-vinylpyrrolidone).[83]

Our group exploited this technique for preparing different compounds such as polyurethanes,[84,85] poly(diurethane

TABLE 1 Composition and Conversions of the Polymer Nanocomposites Prepared in This Study, and Temperatures and Velocities of the Polymerization Fronts

Sample	Graphene Concentration in NVCL (mg/mL)	Graphene Concentration in PNVCL (wt %)	T_{max} (°C)	V_f (cm/min)	Conversion (%)
FP1	0	0	166	1.50	98
FP2	0.1	0.0088	161	1.05	98
FP3	0.2	0.018	166	1.24	99
FP4	0.5	0.044	162	1.40	99
FP5	1.0	0.088	165	1.32	100
FP6	2.0	0.18	165	1.32	100
FP7	5.0	0.44	164	1.03	100

diacrylates),[86] unsaturated polyester/styrene resins,[87] epoxy–amine systems,[88–91] hybrid organic–inorganic epoxy resins,[92] and we prepared phosphonium-based ionic liquids as radical initiators for FP.[93]

FP can be also applied to the synthesis of polymer hydrogels and drug delivery systems: in 2001, Washington and Stainbock demonstrated that the use of FP in the synthesis of PNIPAAm hydrogels allowed obtaining a material characterized by a very narrow pore size distribution. Indeed, as the front temperature increases, some macroscopic phenomena of phase separation, microaggregation and sedimentation of domains having different densities are inhibited.[94] Stimuli responsive hydrogels of poly(*N*,*N*-dimethylacrylamide),[95] poly(acrylamide-co-3-sulfopropyl acrylate),[96] poly(*N*-isopropylacrylamide-co-3-sulfopropyl acrylate),[97] P(NIPAAm-*co*-NVCL),[98] and poly(2-hydroxyethylacrylate-*co*-acrylic acid)[99] were successfully obtained. FP was also exploited for the obtainment of controlled drug-release systems,[100] for stone consolidation,[101,102] and for preparing polymer-based nanocomposites with montmorillonite[103] or polyhedral oligomeric silsesquioxanes.[104] Recently, we have proposed FP for the obtainment of polymer nanocomposites based on poly(tetraethyleneglycoldiacrylate) containing graphene;[52] in addition, some stimuli responsive polymer hydrogels based on PNIPAAm and containing graphene or partially exfoliated graphite have been successfully prepared by FP, as well.[42,105]

Taking into account the above considerations, the present study focuses on the preparation of novel thermoresponsive nanocomposite PNVCL/graphene hydrogels by exploiting FP as the synthetic route. High graphene concentrations in the liquid monomer have been achieved by simply sonicating graphite dispersions in the liquid NVCL monomer; furthermore, the morphology of the obtained hydrogels has been assessed by TEM measurements. Finally, the influence of the nanofiller on the swelling behavior of the obtained hydrogels at different temperatures and on the rheological features has been thoroughly investigated.

EXPERIMENTAL

Materials

N-vinylcaprolactam (NVCL, FW = 139.2, d = 1.029 g/mL) and tetraethyleneglycoldiacrylate (TEGDA, FW = 302.33 g/mol, d = 1.11 g/mL) were purchased from Sigma Aldrich and used as received. Trihexyltetradecylphosphonium persulfate (TETDPPS, FW = 1115) was prepared following the method reported in a previous study.[93] Graphite flakes were purchased from Aldrich and used as received.

Graphene Dispersion Preparation

A graphene masterbatch dispersion was prepared by dispersing 5 wt % graphite flakes in NVCL, placed into a tubular plastic reactor (i.d. 15 mm) and ultrasonicating it for 24 h at 40°C (Ultrasound bath EMMEGI, 0.55 kW). Then, the dispersion was centrifuged for 30 min at 4000 rpm and the gray to black liquid phase containing graphene was recovered. The concentration of the graphene dispersion, obtained by gravimetric filtration through polyvinylidene fluoride filters (pore size 0.22 mm), was 5.0 mg/mL.

Synthesis of Poly(*N*-vinylcaprolactam) Hydrogels

The nanocomposite polymer hydrogels of PNVCL containing graphene were prepared by varying the amount of the nanofiller from 0.0088 to 0.44 wt % (corresponding to 0.1 and 5.0 mg/mL, respectively, referred to NVCL monomer), and keeping constant the amount of crosslinker (TEGDA), and initiator (TETDPPS), both at 1 mol% referred to the amount of NVCL (Table 1).

The graphene masterbatch dispersion in NVCL was diluted with suitable amounts of NVCL, thus obtaining dispersions containing a different concentration of graphene. Each dispersion was poured into a common glass test tube (i.d. = 1.5 cm, length = 16 cm), and added of TEGDA and TETDPPS. A thermocouple was located at about 1 cm from the bottom of the tube and connected to a digital temperature recorder (Delta Ohm 9416, sampling rate: 1 Hz). FP started by heating the external wall of the tube in correspondence of the upper surface of the monomeric mixture. The position of the front (easily visible through the glass wall of test tubes) vs. time was also monitored. For all the samples, front temperature (T_{max}, ±10°C) and front velocity (V_f, ±0.5 cm/min) were measured.

Characterization

The graphene–NVCL masterbatch dispersion was submitted to UV–Vis spectroscopic analysis, using a Hitachi U-2010 spectrometer (1 mm cuvette) and following the method described in the published reports.[106] A calibration curve

was constructed for the wavelength of 660 nm, to evaluate the molar extinction coefficient of the dispersion [which was found to be equal to 1502 mL/(m mg)] and to determine the graphene concentration in all the diluted dispersions derived from the masterbatch.

Raman analyses were performed using a Bruker Senterra Raman microscope with an exciting radiation of 532 nm at 5 mW. The spectra were acquired by averaging five acquisitions of 5 s with a 50× objective.

The morphological characterization of polymer hydrogels was carried out using a SEM Zeiss EVO LS10.

The swelling behavior as a function of temperature of the PNVCL–graphene nanocomposite hydrogels was measured in water from 3 to 55°C using a thermostatic bath. To this aim, three different heating rates were used, namely 3°C/day (from 3 to 9 °C), 1°C/day (from 25 to 35°C), and 5°C/day (from 35 to 55°C). The swelling ratio (SR%) was calculated by the following equation:

$$\mathrm{SR}\% = \frac{M_s - M_d}{M_d} 100$$

where M_s and M_d are the hydrogel masses in the swollen and in the dried state, respectively. The reported data are an average of three measurements (reproducibility was about ±10%).

Rheological measurements were carried out on a strain-controlled rheometer (ARES, TA Instruments, Waters LLC) with a torque transducer range of 0.2–2000 gf cm, using 25 mm parallel plate geometry. Frequency sweep tests were carried out in the linear viscoelastic region for all the samples, at 25°C, 0.1–100 rad/s. Strain has been chosen to have a torque within the sensitivity of the instrument in the linear viscoelastic region. To assure reproducibility, at least four measurements were performed on each sample.

Transmission electron microscopy (TEM) studies were performed on a JEOL JEM-1011 working at an accelerating voltage of 100 kV. Ultrathin sections (nominal thickness of 100 nm) of either dried and swollen hydrogels were cut at −120°C using a Leica Ultracut UCT microtome with a EM-FCS cryo kit equipped with a diamond knife, and collected onto formvar-coated 400 mesh copper grids. The sections from dried samples were difficult to handle because of the accumulated static charge and had to be removed from the knife edge with an eyelash, transferred to a supersaturated sucrose solution and then placed on the grids. In the case of swollen gels, a drop a sucrose solution was used to collect the cuts directly from the microtome and to transfer them to the grids. Finally, the sucrose was washed away with deionized water, and the grids dried at room temperature. Apart from the direct visualization of different graphene morphologies, TEM images were also analyzed to offer a qualitative determination of the amount of isolated few-layer graphene sheets to aggregated graphenes, in a series of at least 10 images per sample.

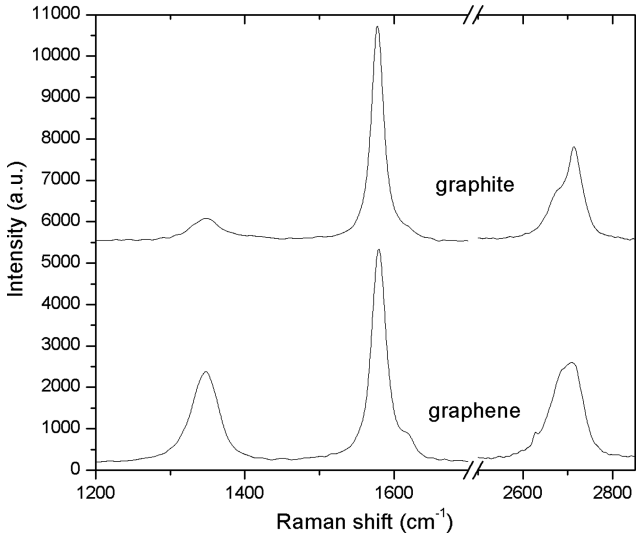

FIGURE 1 Raman spectra of graphene obtained after filtration of the NVCL dispersion (bottom) and pristine graphite (top).

RESULTS AND DISCUSSION

First, graphene dispersions in NVCL were subjected to Raman analysis to confirm the presence of graphene itself and to determine the number of graphene layers.[66,107,108] In Figure 1, a comparison between the Raman spectra of graphite and graphene obtained by gravimetric filtration of its dispersion in NVCL is reported. As can be seen, both the spectra exhibit three typical signals, namely the D band at 1350 cm^{-1}, the G band at 1580 cm^{-1} and the disorder-related 2D peak at a frequency of ca. 2700 cm^{-1}. The 2D band is a diagnostic signal for the identification of graphene because its shape differs from that of graphite: indeed, it can (i) be fully symmetrical (in mono-layer graphene) or (ii) have a shoulder (in graphite), or (iii) be characterized by an intermediate shape depending on the number of layers.

In the example reported in Figure 1, the shape and the position of the 2D band suggest that the sample under examination consists of few-layer graphene, this name referring to graphene flakes made up of five to seven layers. On the contrary, graphite shows a very different 2D band, which consists of two components with a stronger peak at 2713 cm^{-1}.[109] The graphene concentration in NVCL was also estimated using the method reported in previous studies[42,52,69] and was found to be 5.0 mg/mL, one of the highest reported so far in published reports with any method and in any liquid.

From the above graphene dispersions in NVCL, several polymer nanocomposites having graphene concentrations ranging from 0.0088 to 0.44 wt % were prepared by FP. As can be seen in Table 1, front temperatures are not affected by the presence of graphene and T_{max} values are always comprised between 161 and 166°C. At variance, a relatively larger range characterizes front velocities (V_f): namely, the addition of graphene results in decreasing V_f from 1.50 cm/min for the neat polymer to values ranging from 1.03 to 1.40 cm/min for

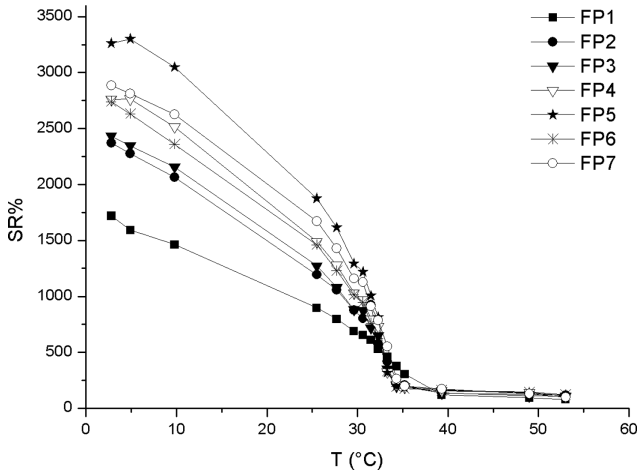

FIGURE 2 SR% as a function of temperature for samples containing different graphene amounts. (see Table 1 for compositions).

the nanocomposites. Since this decrease cannot be easily explained by considering the dissipated heat because of the addition of such an inert component, further study on the possible effect of graphene on this parameter are in progress and will reported soon.

Besides, all the samples showed an almost quantitative conversion, which is independent of graphene concentration and is much higher than that previously reported in the published reports for the classical polymerization of NVCL, performed in solution at 60°C for 192 h (<90%).[110]

The formation of the polymer was confirmed by Raman spectroscopy; namely, the typical PNVCL peaks were found at 700 cm^{-1} (δ—N—C=O), 1447 cm^{-1} (δ—CH_2), 1629 cm^{-1} (ν—C=O), 2927 cm^{-1} (ν—CH_2). Unfortunately, because of the superposition of graphene bands with those of PNVCL, only the peaks of this latter are visible in all the spectra of graphene-containing samples (not shown). This finding confirms the reliability of FP as a convenient alternative polymerization technique.

The swelling ratio of the nanocomposite polymer hydrogels as a function of temperature was measured from 3 to 53°C in a thermostatic bath.

As depicted in Figure 2, at 3°C the swelling ratio is strongly influenced by the concentration of graphene embedded in the nanocomposite hydrogels. Namely, SR% increases from 1700% for the neat polymer to 2400% for the nanocomposite having the lowest graphene content (0.0088 wt %, sample FP2). Such an SR% increase is a clear indication that graphene largely interacts with the polymer matrix, affecting its typical properties even if present in small quantities.

SR% increases with increasing graphene content and reaches a maximum value (3300%) for the hydrogel containing 0.088 wt % graphene (sample FP5). Furthermore, the increase of SR% as graphene increases may be attributed to the disturbance of this nanoparticle on the crosslinking occurrence.

On the other hand, when graphene concentration exceeds 0.088 wt %, SR% decreases down to 2700% (for sample FP6, which contains 0.18 wt % graphene) and to 2900% (sample FP7, which contains 0.44 wt % graphene). This last finding might be related to the decrease of the whole hydrophilic character of the nanocomposite polymer hydrogel, which, in turns, can be attributable to the presence of the relatively large amount of highly hydrophobic graphene sheets. Furthermore, the nanofiller does not affect the LCST, always located at ca. 32–33°C, a value that is close to the physiological one.

The dispersion state of the graphene sheets and the morphological structure of the polymer nanocomposite hydrogels were assessed by TEM and SEM, respectively. As shown in TEM images, the nanofiller consists of flakes with an average length below 1 μm and a number of sheets roughly evaluated from the edges, which tend to fold back in between two and several layers [Fig. 3(a,b)]. The ratio of isolated to aggregated graphene sheets was difficult to evaluate over very large areas, mainly because of the big difference of contrast and brightness. Nevertheless, approximately 1 μm-size graphene particle [example in Fig. 3(c)] any tens of well-dispersed structures was observed. The concentration of such graphene granes in ultra-microtomed samples from dried hydrogel was qualitatively higher than in those obtained by direct cryogenic sectioning of the swollen gel. This finding possibly indicates that aggregation takes place during the drying process, as a direct consequence of shrinkage, especially in the case of bulk samples. As a matter of fact, such tendency was more apparent for nanocomposites having a higher graphene content, and especially for sample FP7.

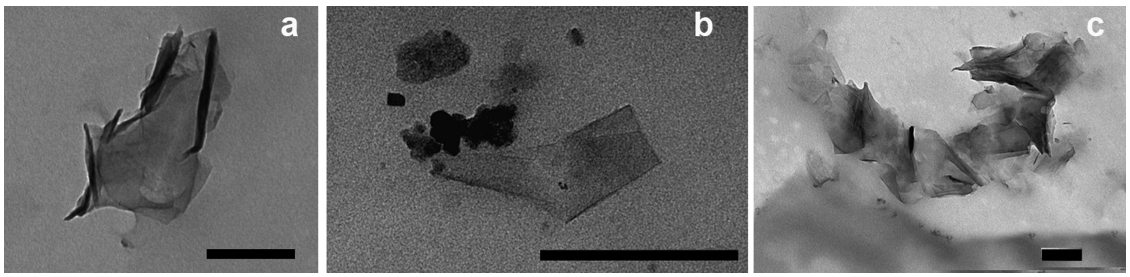

FIGURE 3 TEM images of few layer graphene sheets (a,b) and a graphene aggregate (c) in sample FP7. Scale bar: 200 nm.

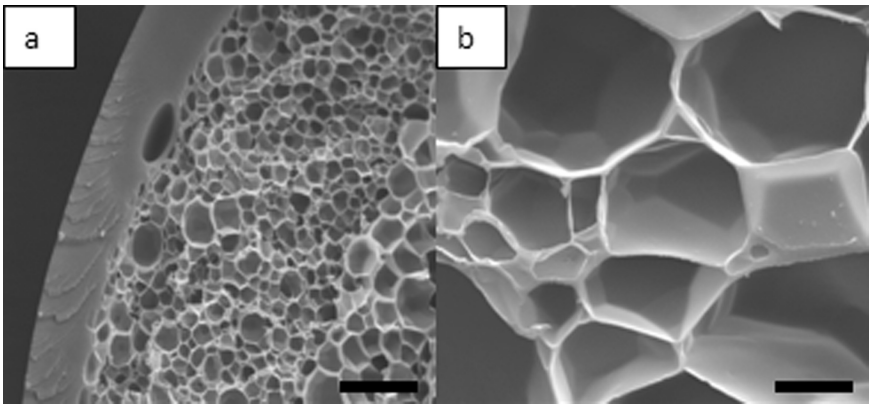

FIGURE 4 SEM micrographs of: (a) sample FP1 (neat polymer), and (b) sample FP2 (containing 0.0088 wt % graphene). Scale bar: 200 nm.

The morphological structure of the obtained polymer nanocomposite hydrogels was investigated by SEM. First, it had to be noticed that this technique does not allow detecting the presence of graphene; furthermore, both the neat polymer (sample FP1) and the nanocomposites show a highly micro-porous structure (see Fig. 4). It is worthy to note that the pore diameters of the neat polymer [sample FP1, Fig. 4(a)] are much smaller than those of graphene-containing hydrogels [sample FP2, Fig. 4(b)]. This difference may be attributed to the presence of graphene sheets, which partially disturb the crosslinking. This assumption is in agreement with what stated above about the influence of graphene in the swelling behavior of the prepared hydrogels.

As far as the rheological characterization is concerned, Figure 5(a) plots the storage modulus (G') as a function of frequency for neat PNVCL and some PNVCL/graphene hydrogels. The neat polymer shows the presence of a horizontal plateau, which refers to a typical crosslinked material. The presence of the filler does not affect the elastic response of all the tested compositions: indeed, G' remains constant within the frequencies range explored.

The lubrication effect induced by graphene sheets, which has been already observed for other polymer matrices,[42] promotes a decrease of G' with increasing graphene content [Fig. 5(a)]: unlike PNIPAAm hydrogels,[42] a threshold filler concentration is not present in the systems under study, so that the complex viscosity curves are continuously shifted toward lower values with increasing the nanofiller content [Fig. 5(b)].

Furthermore, the slope of the regression lines, which gives an indication of the non-Newtonian behavior of the hydrogels, is in the same range (~0.95) for all the compositions investigated and further confirms the unchanged viscoelastic behavior of all the nanocomposites with respect to the unfilled counterpart.

CONCLUSIONS

In the present study, FP was successfully exploited for the synthesis of thermoresponsive graphene-based poly(*N*-vinylcaprolactam) nanocomposite hydrogels. This is the first time that NVCL was frontally polymerized; furthermore, the monomer to polymer conversions were always

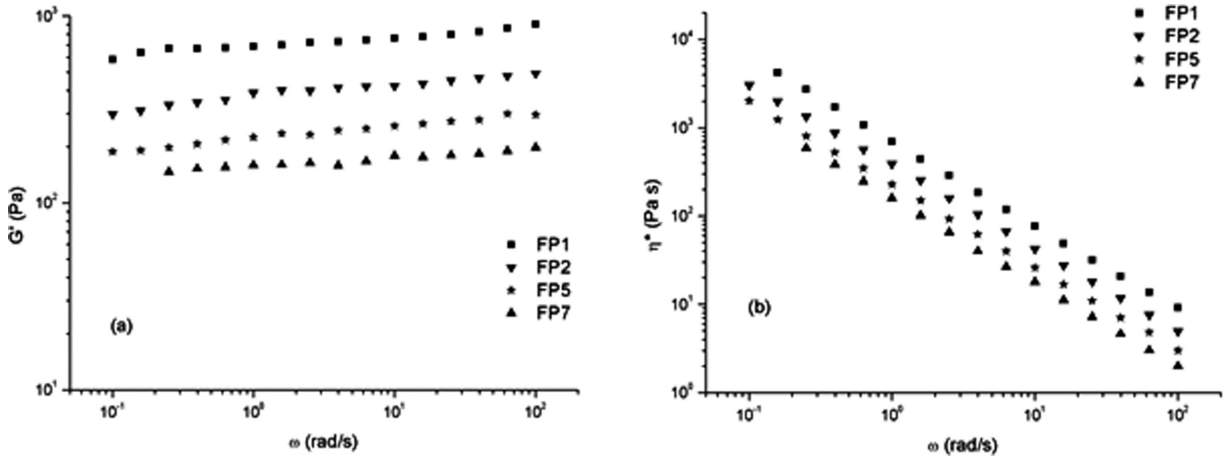

FIGURE 5 (a) Storage modulus G' and (b) complex viscosity as a function of frequency for some investigated PNVCL (see Table 1 for compositions).

almost quantitative, thus confirming the feasibility of FP in the easy, short time consuming macromolecular synthesis.

At variance to the most commonly reported methods, which are more complicated and often less effective, the one used in the present study easily allows obtaining defect-free graphene by direct graphite sonication. In particular, when compared with the other route for obtaining graphene in liquid dispersion, which consists of graphite oxide partial reduction, no chemical modification was used, thus achieving "real" graphene. Besides, the utilized dispersing medium was the self-same liquid monomer. In such a method, the graphene/monomer dispersion was directly polymerized to achieve the corresponding nanocomposites, thus avoiding solvent removal, which is a process that may result in graphene aggregation to form graphite. Graphene concentration in NVCL was one of the highest reported so far in published reports using any method and any liquid (5.0 mg/mL).

As far as the material properties are concerned, it is noteworthy that graphene influences the swelling ratio of the obtained hydrogels; namely, at 3°C, SR% ranges from between 1700% for the neat polymer to 3260% for one of the graphene-containing nanocomposites. However, all the materials exhibit the same LCST at ca. 32–33°C, independently of the presence of graphene and its concentration. Furthermore, similarly to what already reported in Ref. 42, the study on the rheological properties evidenced that the G' modulus and complex viscosity of the hydrogels decrease as the amount of nanofiller increases, thus indicating that graphene exerts a lubrication effect.

REFERENCES AND NOTES

1 Park, K. Biodegradable Hydrogels for Drug Delivery; CRC Press, Lancaster, **1993.**

2 Liu, Z. S.; Calvert, P. *Adv. Mater.* **2000,** *12*, 288–291.

3 Liu, T. Y.; Hu, S. H.; Liu, D. M.; Chen S. Y.; Chen, W. I. *Nano Today* **2009,** *4*, 52–65.

4 Gupta, P.; Vermani, K.; Garg, S. *Drug Discov. Today* **2002,** *7*, 569–579.

5 Jeong, B.; Gutowska, A. *Trends Biotechnol.* **2002,** *20*, 305–331.

6 Jhaveri, S. J.; Hynd, M. R.; Dowell-Mesfin, N.; Turner, J. N.; Shain, W.; Oberet, K. *Biomacromolecules* **2009,** *10*, 174–183.

7 Hoffman, A. S. *J. Control. Release* **2008,** *132*, 153–163.

8 Barker, S. L. R.; Ross, D.; Tarlov, M. J.; Gaitan M.; Locascio, L. E. *Anal. Chem.* **2000,** *72*, 5925–5929.

9 Kikuchi, A.; Okano, T. *Adv. Drug Deliv. Rev.* **2002,** *54*, 53–77.

10 Li, S. K.; D'Emanuele, A. *J. Control. Release* **2001,** *75*, 55–67.

11 Hoffmann, J.; Plotner, M.; Kuckling D.; Fischer, W. J. *Sens. Actuators A* **1999,** *77*, 139–140.

12 Ista, L. K.; Lopez, G. P. *J. Ind. Microbiol. Biotechnol.* **1998,** *20*, 121–125.

13 Cunliffe, D.; De las Heras Alarcon, C.; Peters, V.; Smith, J. R.; Alexander, C. *Langmuir* **2003,** *19*, 2888–2899.

14 Schild, H. G. *Prog. Polym. Sci.* **1992,** *17*, 163–249.

15 Li, X.; Liu, W.; Ye, G.; Zhang, B.; Zhu, D.; Yao, K.; Liu, Z.; Sheng, X. *Biomaterials* **2005,** *26*, 7002–7011.

16 Yoshida, R.; Uchida, K.; Kanecko, Y.; Sakai, K.; Kikuchi, A.; Sakurai, Y.; Okano, T. *Macromolecules* **1991,** *24*, 549–551.

17 Serres, A.; Baudys, M.; Kim, S.W. *Pharm. Res.* **1996,** *13*, 196–201.

18 Ramkissoon-Ganorkar, C.; Liu, F.; Baudys, M.; Kim, S.W. *J. Biomater. Sci. Polym. Ed.* **1999,** *10*, 1149–1161.

19 Van Durme, K.; Verbrugghe, S.; Du Prez, F.E.; Van Mele, B. *Macromolecules* **2004,** *37*, 1054–1061.

20 Makhaeva, E. E.; Tenhu, H.; Khokhlov, A.R. *Macromolecules* **1998,** *31*, 6112.

21 Eisele, M.; Burchard, W. *Makromol. Chem.* **1990,** *191*, 169–184.

22 Mikheeva, L. M., Grinberg, N. V.; Mashkevich, A. Y.; Grinberg, V. Y.; Thanh, L. T. M.; Makhaeva, E. E.; Khokhlov, A. R. *Macromolecules* **1997,** *30*, 2693–2699.

23 Kirsh, Y. E. Water Soluble Poly-N-vinylamides; Wiley: Chichester, **1998, pp 1–33.**

24 Davidenko, T. I.; Shapiro, Y. E.; Kravchenko, I. A.; Sevastyanov, O. V.; Gorbatyuk V. Y.; Krasnoshchekaya, S. P. *Russ. Chem. Bull.* **1996,** *45*, 2136–2140.

25 Davidenko, T. I.; Akhmed, K. A. *Khim. Tekhnol. Vody* **2001,** *23*, 142–149.

26 Lau A. C. W.; Wu, C.; *Macromolecules* **1999,** *32*, 581–584.

27 De las Heras Alarcòn, C.; Pennadam, S.; Alexander, C. *Chem. Soc. Rev.* **2005,** *34*, 276–285.

28 Imaz, A.; Formacada, J. *J. Polym. Sci. Part A: Polym. Chem.* **2010,** *48*, 1173–1181.

29 Kirsh, Y. E. In: Water Soluble Poly-N-vinylamides; Wiley: Chichester, **1998,** pp 186–189.

30 Mardyani, S.; Chan, W. C. W.; Kumacheva, E. *Adv. Mater.* **2006,** *18*, 80–83.

31 Soppimath, K. S.; Tan, D. C. W.; Yang, Y. *Adv. Mater.* **2005,** *17*, 318–323.

32 Guiseppi-Elie, A.; Sheppard, N. F.; Brahim, S.; Narinesingh, D. *Biotechnol. Bioeng* **2001,** *75*, 475–484.

33 Kawaguchi, H.; Fujimoto, K. S. *Bioseparation* **1998,** *4*, 253–258.

34 Nelson, A.; Cosgrove, T. *Langmuir* **2004,** *20*, 10382–10388.

35 Loizou, E.; Butler, P.; Porcar, L.; Kesselman, E.; Talmon, Y.; Dundigalla, A.; Schmidt, G. *Macromolecules* **2005,** *38*, 2047–2049.

36 Mohan, Y. M.; Premkumar, T.; Lee, K.; Geckeler, K. E. *Macromol. Rapid Commun.* **2006,** *27*, 1346–1354.

37 Sahiner, N. *Colloid Polym. Sci.* **2006,** *285*, 283–292.

38 Monticelli, O.; Mendichi, R.; Bisbano, S.; Mariani, A.; Russo, S. *Macromol. Chem. Phys.* **2000,** *201*, 2123–2127.

39 Cohen Stuart, M. A. *Colloid Polym. Sci.* **2008,** *286*, 855–864.

40 Satarkar, N. S.; Zach Hilt, J. *Acta Biomater.* **2008,** *4*, 11–16.

41 Liu, T. Y.; Hu, S. H.; Liu, K. H.; Liu, D. M.; Chen, S. Y. *J. Control. Release* **2008,** *126*, 228–236.

42 Alzari, V.; Nuvoli, D.; Scognamillo, S.; Piccinini, M.; Gioffredi, E.; Malucelli, G.; Marceddu, S.; Sechi, M.; Sanna, V.; Mariani, A. *J. Mater. Chem.* **2011,** *21*, 8727–8733.

43 Slonczewski, J. C.; Weiss, P. R. *Phys. Rev.* **1958,** *109*, 272–279.

44 Bolotin, K. I.; Sikes, K. J.; Jiang, Z.; Klima, M.; Fudenberg, G.; Hone, J.; Kim, P.; Stormer, H. L. *Solid State Commun.* **2008,** *146*, 351–355.

45 Novoselov, K. S.; Geim, A. K.; Morozov, S. V.; Jiang, D.; Katsnelson, M. I.; Grigorieva, I. V.; Dubonos, S.; Firsov, A. A. *Nature* **2005,** *438*, 197–200.

46 Novoselov, K. S.; Geim, A. K.; Morozov, S. V.; Jiang, D.; Zhang, Y.; Dubonos, S. V.; Grigorieva, I. V.; Firsov, A. A. *Science* **2004,** *306*, 666–669.

47 Wu, J.; Becerril, H. A.; Bao, Z.; Liu, Z.; Chen, Y.; Peumans, P. *Appl. Phys. Lett.* **2008,** *92*, 263302.

48 Liu, Z. F.; Liu, Q.; Huang, Y.; Ma, Yin, Y. F. S. G.; Zhang, X. Y.; Sun, W.; Chen, Y. S. *Adv. Mater.* **2008,** *20*, 3924–3930.

49 Gilje, S.; Han, S.; Wang, M.; Wang, K. L.; Kaner, R. B. *Nano Lett.* **2007,** *7*, 3394–3398.

50 Schedin, F.; Geim, A. K. S.; Morozov, V.; Hill, E.; Blake, W. P.; Katsnelson, M. I.; Novoselov, K. S. *Nat. Mater.* **2007,** *6*, 652–655.

51 Lee, C.; Wei, X.; Kysar, J. W.; Hone, J. *Science* **2008,** *321*, 385–388.

52 Alzari, V.; Nuvoli, D.; Sanna, R.; Scognamillo, S.; Piccinini, M.; Kenny, J. M.; Malucelli, G.; Mariani, A. *J. Mater. Chem.* **2011,** *21*, 16544–16549.

53 Lee, S.; Lee, K.; Zhong, Z. *Nano Lett* **2010,** *10*, 4702–4707.

54 Valentini, L.; Trentini, M.; Mengoni, F.; Alongi, J.; Armentano, I.; Ricco, L.; Mariani, A.; Kenny, J. M. *Diam. Relat. Mater.* **2007,** *16*, 658–663.

55 Xianbao, W.; Haijun, Y.; Fangming, L.; Mingjian, L.; Li, W.; Shaoqing, L.; Qin, L.; Yang, X.; Rong, T.; Ziyong, Y.; Dong, X.; Jing, C. *Chem. Vap. Deposition* **2009,** *15*, 53–66.

56 Kim, C. D.; Min, B. K.; Jung, W. S. *Carbon* **2009,** *47*, 1610–1612.

57 Stankovich, S; Dikin, D. A.; Piner, R. D.; Kohlhaas, K. A.; Kleinhammes, A.; Jia, Y.; Wu, Y.; Nguyen, S. T.; Ruoff, R. S. *Carbon* **2007,** *45*, 1558–1565.

58 Stankovich, S.; Dikin, D. A.; Dommett, G. H. B.; Kohlhaas, K. M.; Zimney, E. J.; Stach, E. A.; Piner, R. D.; Nguyen, S. T.; Ruoff, R. S. *Nature* **2006,** *442*, 282–286.

59 Verdejo, R.; Barroso-Bujans, F.; Rodriguez-Perez, M. A.; De Saja, J. A.; Lopez-Manchado, M. A. *J. Mater. Chem.* **2008,** *18*, 2221–2226.

60 Russo, S.; Mariani, A.; Ignatov, V. N.; Ponomarev, I. I. *Macromolecules* **1993,** *26*, 4984–4985.

61 Schniepp, H. C.; Li, J. L.; McAllister, M. J.; Sai, H.; Herrera-Alonso, M.; Adamson, D. H.; Prud'homme, R. K.; Car, R.; Saville, D. A.; Aksay, I. A. *J. Phys. Chem. B* **2006,** *110*, 8535–8339.

62 Forbeaux, I.; Themlin, J. M.; Debever, J. M. *Phys. Rev. B* **1998,** *58*, 16396–16406.

63 Han, M. Y.; Ozyilmaz, B.; Zhang, Y.; Kim, P. *Phys. Rev. Lett.* **2007,** *98*, 206805–206809.

64 Barone, V.; Hod, O.; Scuseria, G. E. *Nano Lett.* **2006,** *6*, 2748–2754.

65 Li, N.; Wang, Z.; Zhao, K.; Shi, Z.; Gu, Z.; Xu, S. *Carbon* **2009,** *48*, 255–259.

66 Karmakar, S.; Kulkarni, N. V.; Nawale, A. B.; Lalla, N. P.; Mishra, R.; Sathe, V. G.; Bhoraskar, S. V.; Das, A. K. *J. Phys. D: Appl. Phys.* **2009,** *42*, 115201/1–11501/14.

67 Hernandez, Y.; Nicolosi, V.; Lotya, M.; Blighe, F. M.; Sun, Z.; De, S.; McGovern, I. T.; Holland, B.; Byrne, M.; Gun'Ko, Y. K.; Boland, J. J.; Niraj, P.; Duesberg, G.; Krishnamurthy, S.; Goodhue, R.; Hutchison, J.; Scardaci, V.; Ferrari, A. C.; Coleman, J. N. *Nat. Nanotechnol.* **2008,** *3*, 563–568.

68 Lotya, M.; Hernandez, Y.; King, P. J.; Smith, R. J.; Nicolosi, V.; Karlsson, L. S.; Blighe, F. M.; De, S.; Wang, Z.; McGovern, I. T.; Duesberg, G. S.; Coleman, J. N. *J. Am. Chem. Soc.* **2009,** *131*, 3611–3620.

69 Nuvoli, D.; Valentini, L.; Alzari, V.; Scognamillo, S.; Bittolo Bon, S.; Piccinini, M.; Illescasd, J.; Mariani, A. *J. Mater. Chem.* **2011,** *21*, 3428–3431.

70 Chechilo, N. M.; Enikolopyan, N. S.; *Dokl. Phys. Chem.* **1975,** *221*, 392–394.

71 Chechilo, N. M.; Enikolopyan, N. S. *Dokl. Phys. Chem.* **1976,** *230*, 840–843.

72 Pojman, J. A. *J. Am. Chem. Soc.* **1991,** *113*, 6284–6286.

73 Pojman, J. A.; Craven, R.; Khan, A.; West, W. W. *J. Phys. Chem* **1992,** *96*, 7466–7472.

74 Pojman, J. A.; Willis, J. R.; Forthenberry, D.; Ilyashenko, V.; Khan, A. M. *J. Polym. Sci. Part A: Polym. Chem.* **1995,** *33*, 643–652.

75 Chekanov, Y.; Arrington, D.; Brust, G.; Pojman, J. A. *J. Appl. Polym. Sci.* **1997,** *66*, 1209–1216.

76 Scognamillo, S.; Bounds, C.; Luger, M.; Mariani, A.; Pojman, J. A. *J. Polym. Sci. Part A: Polym. Chem.* **2010,** *48*, 2000–2005.

77 Jiménez, Z.; Pojman, J. A. *J. Polym. Sci. Part A: Polym. Chem.* **2007,** *45*, 2745–2754.

78 Pojman, J. A.; Elcan, W.; Khan, A. M.; Mathias, L. *J. Polym. Sci. Part A: Polym. Chem.* **1997,** *35*, 227–230.

79 Mariani, A.; Fiori, S.; Chekanov, Y.; Pojman, J. A. *Macromolecules* **2001,** *34*, 6539–6541.

80 Hu, T.; Chen, S.; Tian, Y.; Chen, L.; Pojman, J. A. *J. Polym. Sci. Part A: Polym. Chem.* **2007,** *45*, 873–881.

81 Chen, L.; Hu, T.; Yu, H.; Chen, S.; Pojman, J. A. *J. Polym. Sci. Part A: Polym. Chem.* **2007,** *45*, 4322–4330.

82 Chen, S.; Tian, Y.; Chen, L.; Hu, T. *Chem. Mater.* **2006,** *18*, 2159–2163.

83 Cai, X.; Chen, S.; Chen, L. *J. Polym. Sci. Part A: Polym. Chem.* **2008,** *46*, 2177–2185.

84 Mariani, A.; Bidali, S.; Fiori, S.; Malucelli, G.; Sanna, E. *e-Polymers* **2003,** *44*, 1–9.

85 Fiori, S.; Mariani, A.; Ricco, L.; Russo, S. *Macromolecules* **2003,** *36*, 2674–2679.

86 Mariani, A.; Fiori, S.; Bidali, S.; Alzari, V.; Malucelli, G. *J. Polym. Sci. Part A: Polym. Chem.* **2008,** *46*, 3344–3351.

87 Fiori, S.; Malucelli, G.; Mariani, A.; Ricco, L.; Casazza, E. *e-Polymers* **2002,** *57*, 1–10.

88 Frulloni, E.; Salinas, M. M.; Torre, L.; Mariani, A.; Kenny, J. M. *J. Appl. Polym. Sci.* **2005,** *96*, 1756–1766.

89 Mariani, A.; Bidali, S.; Caria, G; Monticelli, O.; Russo, S.; Kenny, J. M. *J. Polym. Sci. Part A: Polym. Chem.* **2007,** *45*, 2204–2211.

90 Mariani, A.; Bidali, S.; Fiori, S.; Sangermano, M.; Malucelli, G.; Bongiovanni, R.; Priola, A. *J. Polym. Sci. Part A: Polym. Chem.* **2004,** *42*, 2066–2072.

91 Mariani, A.; Alzari, V.; Monticelli, O.; Pojman, J. A.; Caria, G. *J. Polym. Sci. Part A: Polym. Chem.* **2007,** *45*, 4514–4521.

92 Scognamillo, S., Alzari, V.; Nuvoli, D.; Mariani, A. *J. Polym. Sci. Part A: Polym. Chem.* **2010,** *48*, 4721–4725.

93 Mariani, A.; Nuvoli, D.; Alzari, V.; Pini, M. *Macromolecules* **2008,** *41*, 5191–5196.

94 Washington, R. P.; Steinbock, O. *J. Am. Chem. Soc.* **2001,** *123*, 7933–7934.

95 Caria, G.; Alzari, V.; Monticelli, O.; Nuvoli, D.; Kenny, J. M.; Mariani, A. *J. Polym. Sci. Part A: Polym. Chem.* **2009,** *47*, 1422–1428.

96 Scognamillo, S.; Alzari, V.; Nuvoli, D.; Mariani, A. *J. Polym. Sci. Part A: Polym. Chem.* **2010,** *48*, 2486–2490.

97 Scognamillo, S.; Alzari, V.; Nuvoli, D.; Illescas, J.; Marceddu, S.; Mariani, A. *J. Polym. Sci. Part A: Polym. Chem.* **2011,** *49*, 1228–1234.

98 Alzari, V.; Monticelli, O.; Nuvoli, D.; Kenny, J. M.; Mariani, A. *Biomacromolecules* **2009,** *10*, 2672–2677.

99 Sanna, R.; Alzari, V.; Nuvoli, D.; Scognamillo, S.; Marceddu, S.; Mariani, A. *J. Polym. Sci. Part A: Polym. Chem.* **2012,** *50*, 1515–1520.

100 Gavini, E.; Mariani, A.; Rassu, G.; Bidali, S.; Spada, G.; Bonferoni, M. C.; Giunchedi, P. *Eur. Polym. J.* **2009,** *45*, 690–699.

101 Brunetti, A.; Princi, E.; Vicini, S.; Pincin, S.; Bidali, S.; Mariani, A. *Nucl. Instrum. Meth. B* **2004,** *222*, 235–241.

102 Vicini, S.; Mariani, A.; Princi, E.; Bidali, S.; Pincin, S.; Fiori, S.; Pedemonte, E.; Brunetti, A. *Polym. Adv. Technol.* **2005,** *16*, 293–298.

103 Mariani, A.; Bidali, S.; Caria, G.; Monticelli, O.; Russo, S.; Kenny, J. M. *J. Polym. Sci. Part A: Polym. Chem.* **2007,** *45*, 2204–2211.

104 Mariani, A.; Alzari, V.; Monticelli, O.; Pojman, J. A.; Caria, G. *J. Polym. Sci. Part A: Polym. Chem.* **2007,** *45*, 4514–4521.

105 Alzari, V.; Mariani, A.; Monticelli, O.; Valentini, L.; Nuvoli, D.; Piccinini, M.; Scognamillo, S.; Bon, S. B.; Illescas, J. *J. Polym. Sci. Part A: Polym. Chem.* **2010,** *48*, 5375–5381.

106 Green, A. A.; Hersam, M. C. *Nano Lett.* **2009,** *9*, 4031–4036.

107 Ferrari, A. C. *Solid State Commun.* **2007,** *143*, 47–57.

108 Ferrari, A. C.; Meyer, J. C.; Scardaci, V.; Casiraghi, C.; Lazzeri, M.; Mauri, F.; Piscanec, S.; Jiang, D.; Novoselov, K. S.; Roth, S.; Geim, A. K. *Phys. Rev. Lett.* **2006,** *97*, 187401/1–187401/4.

109 Sun, Z.; Hasan, T.; Torrisi, F.; Popa, D.; Privitera, G.; Wang, F.; Bonaccorso, F.; Basko, D. M.; Ferrari, A. C. *ACS Nano* **2010,** *4*, 803–810.

110 Kozanoglu, S.; Ozdemir, T.; Usanmaz, A.; *J. Macromol. Sci. A Pure Appl. Chem.* **2011,** *48*, 467–477.